AIAA AVIATION Forum
June 27-July 1, 2022, Chicago, IL & Virtual
AIAA AVIATION 2022 Forum

10.2514/6.2022-3737

An aircraft design workflow using the automatic knowledge-based modelling tool JPAD Modeller

V. Trifari[1], A. De Marco[2], M. Di Stasio[3], M. Ruocco[4], F. Nicolosi[5] and G. Grazioso.[6]
University of Naples Federico II, Naples, 80125, Italy

V. Ahuja[7], R. J. Hartfield[8]
Research in Flight, Austin, Texas, USA 78641

Abstract

This paper describes the integrated workflow implemented inside the knowledge-based design tool JPAD Modeller to couple aircraft modelling and aerodynamic analyses using the software FlightStream®. This work aims at showing how to enable aircraft designers to speed up design tasks related both to the modelling and to the aerodynamic assessment of a complete aircraft by providing fast and reliable feedbacks starting from the conceptual and preliminary design phase. A case study concerning the generation, the modification and the aerodynamic analysis of a turboprop commuter aircraft will be shown, also reporting the amount of time required to complete the workflow as well as providing some details on the level of accuracy of the aerodynamic solver used for this type of applications.

I. Introduction

The process of integrating aircraft modelling software and analysis tools in multidisciplinary design workflows plays a fundamental role in the modern aircraft design scenario.

The continuous evolution of computer calculation capabilities has allowed the growth of a large family of software dedicated to aircraft preliminary design activities which usually involve several aircraft design disciplines and allow to carry out complex Multi-Disciplinary Analysis and Optimization (MDAO) workflows.

Nowadays, MDAO workflows are widely used in aircraft preliminary design to solve problems including a large number of parameters and with a strong interaction between many disciplines. In addition, the need to speed up the overall design process to shorten the time-to-market of new aircraft requires that these workflows must provide reliable results in a short period of time.

A first attempt to solve MDAO problems expects to entrust all the analyses to an expert well versed in all disciplines to reduce communications and organization problems. This approach, named Monolithic Design (MD), has been widely used to carry out conceptual design phases in the past and is suitable only for simple problems or when approximate results are acceptable. Nowadays a single expert is unable to monitor a complex process, like the design of a complete aircraft, and new multidisciplinary design techniques are required. To manage all disciplines, a

[1] Post-doctoral researcher, Dept. of Industrial Engineering, vittorio.trifari@unina.it.
[2] Associate Professor, Dept. of Industrial Engineering, agostino.demarco@unina.it.
[3] PhD Student, Dept. of Industrial Engineering, mario.distasio@unina.it.
[4] Post-doctoral researcher, Dept. of Industrial Engineering, manuela.ruocco@unina.it.
[5] Full Professor, Dept. of Industrial Engineering, fabrizio.nicolosi@unina.it, AIAA Member.
[6] Master's degree student, Dept. of Industrial Engineering, giu.grazioso@studenti.unina.it.
[7] CEO, Research in Flight, vivek.ahuja@researchinflight.com.
[8] Co-founder, Research in Flight, roy.hartfield@researchinflight.com.

way could be to define a process in which the aircraft is designed thanks to the collaboration of a group of different experts (one per discipline). This is the Collaborative Design (CD) approach [1]. An example is represented by the Collaborative Remote Design (CRD) approach implemented in the framework of the EU AGILE project [2].

In a very similar way, preliminary aircraft design tools are evolving to deliver more efficient integration environments and to provide ever more fast, reliable and specialized analysis capabilities suitable to include experts' contributions in collaborative design workflows. A remarkable example is represented by the FlightStream® software, a surface vorticity flow solver designed to allow users to develop optimized designs for compressible and incompressible subsonic vehicles as well as transonic vehicles [3].

II. JPAD Modeller

Typically, most of the analysis tools used in modern aircraft design workflows requires an initial aircraft geometry to start an analysis. The generation process of a complete aircraft parametric model suitable for different types of analyses and with an adequate level of detail of its geometry is often a very time-consuming task, mostly handmade. For example, CFD analysis usually requires very detailed aircraft geometries, typically by means of a CAD models shaped in 3D modelling tools like CATIA[4] or SolidWorks[5]. However, since their focus is only on the geometry, those models are not suitable for aircraft preliminary design applications and cannot be included "as is" in a multidisciplinary analysis workflow.

On the other hand, tools like OpenVSP [6] or CPACS Creator [7] allow to easily shape any kind of aircraft geometry from scratch using a parametric model and, in case of CPACS Creator, to include it inside a Collaborative Remote Design workflow using the CPACS file format [8]. However, the level of geometrical detail reached by those models is often not suitable for detailed CFD aerodynamic analyses.

In both cases, the aircraft generation process often lacks a knowledge-based approach to provide the designer with useful feedbacks concerning both the geometrical feasibility of the model and the matching of a given set of Top-Level Aircraft Requirements (TLAR). Thus, a user-friendly aircraft modelling tool including a high level of geometrical detail, a knowledge-based conceptual design approach and the possibility to be easily interconnected to external analysis software and toolchains can be a valid resource for aircraft designers to reduce the time-to-market of new aircraft models.

This paper aims at providing a comprehensive overview of the workflow developed by authors to link an automatic knowledge-based aircraft modelling tool, named JPAD Modeller, with the FlightStream® software to enable users to speed up preliminary design tasks related both to the modelling and to the aerodynamic assessment of a complete aircraft.

The JPAD Modeller software, is the first standalone product of the JPAD software family developed at the University of Naples Federico II by the DAF Research group and commercialized by SmartUp Engineering s.r.l., an academic spin-off company of the University of Naples Federico II [1][9][10][11]. An introduction to the possibilities provided by JPAD Modeller in terms of aircraft geometry modeling is provided in [12], focusing on the capability to automatically generate a fully exportable 3D model.

Coming with a simple and intuitive User Interface (UI), JPAD Modeller allows to generate and manage a parametrically defined aircraft and their CAD models (Fig. 1), as well as to export them in several file formats. Each main aircraft component (lifting surfaces, fuselage, cabin, engines, movables) can be customized according to a pre-selected set of input parameters which have been designed to allow an adequate level of flexibility while keeping the number of input variables at the minimum. In addition, several geometrical update strategies have been implemented to ease the work of the designer and to allow for the modification of more than one input variable at a time, according to precise update rules.

By providing useful aircraft design information and by performing automatic online geometry consistency checks, JPAD Modeller allows to speed up typical handmade industrial processes related to the setup of a baseline aircraft geometry and provides for a robust parametric model that can be imported by external CAD, CFD, and aircraft design tools. Thus, JPAD Modeller represents an efficient pre-processor for some of the most used software typically adopted during aircraft conceptual and preliminary design phases.

Thanks to its Pre-Design module, JPAD Modeller allows to initialize a generic aircraft model starting from a very limited set of information including the set of TLAR, the aircraft category, the mission profile and some high-level aerodynamic input data. Moreover, as shown in Fig. 2, by including a preliminary weights estimation and the possibility to shape the geometry according to a sizing point selected from the feasible zone of the sizing limitations diagram [13], JPAD Modeller allows to increase the level of knowledge since the conceptual design phase.

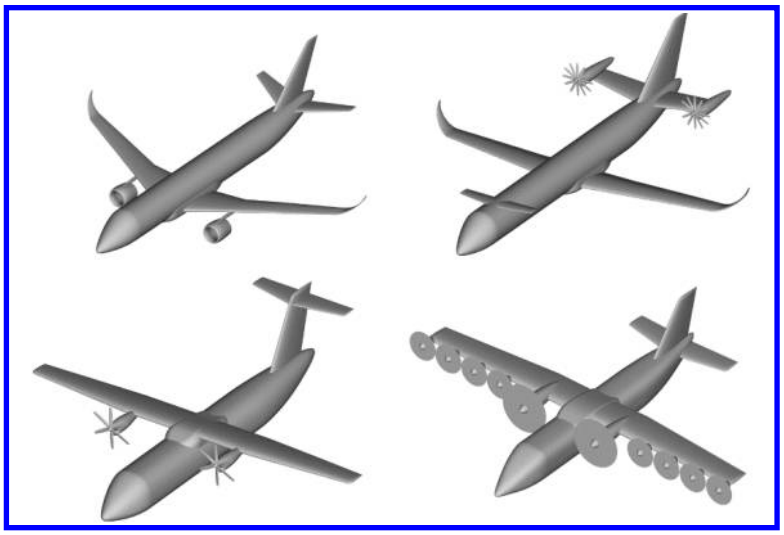

Fig. 1 Different airplanes CAD model automatically generated using JPAD Modeller

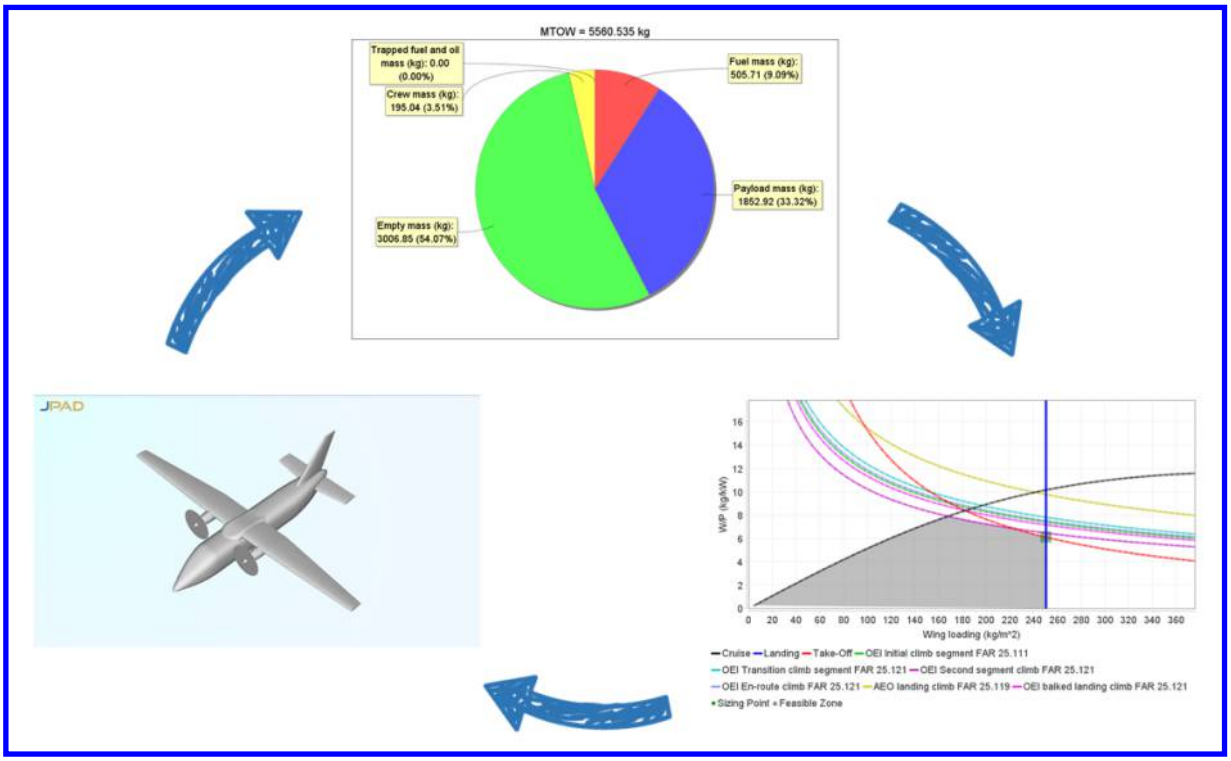

Fig. 2 JPAD Modeller PreDesign module iterative workflow

At this conceptual design stage, the aircraft weight is assumed as follow:

$$W_{TO} = W_e + W_{crew} + W_{payload} + W_{fuel} + W_{tfo} \tag{1}$$

Weight contributions originated from this statistical equation depends on the aircraft class and they are affected by factors related to technological innovation such as, for example, the use of unconventional materials or the adoption of solutions that allow to obtain higher payload capacities.

The Maximum Take-Off Weight (W_{TO}) and Empty Weight (W_e) are calculated from the following equations system:

$$\begin{cases} W_e = W_{to} \cdot c - d \\ W_e = log_{10}{}^{-1}\left(\frac{log_{10}(W_{TO}) - a}{b}\right) \end{cases} \tag{2}$$

Here *a*, *b*, *c*, *d* coefficients are taken from internal JPAD Modeller statistics based on existing aircraft of a given category (e.g., transport jets, regional turboprops, turboprop commuters and business jets). The fuel contribution to the weight estimation comes from statistics as well for all mission phases except the ones related to cruise, alternate and holding for which Breguet equations are adopted.

Usually, typical conceptual design tools and workflows expects that the user assumes reasonable values for the aerodynamic efficiency of the aircraft to be used inside Breguet equations. Conversely, JPAD Modeller allows the user to calculate them starting from an initial estimation of aerodynamic drag polar curves. In particular, the value of the aerodynamic efficiency is evaluated for the different unknown phases depending on the aircraft type assigned in the set of TLAR. Starting from the definition of the lift coefficients for each characteristic points of the parabolic drag polar curve (point E, point A and point P in Fig. 3), a summary of all the assumptions implemented in JPAD Modeller is provided in Table 1.

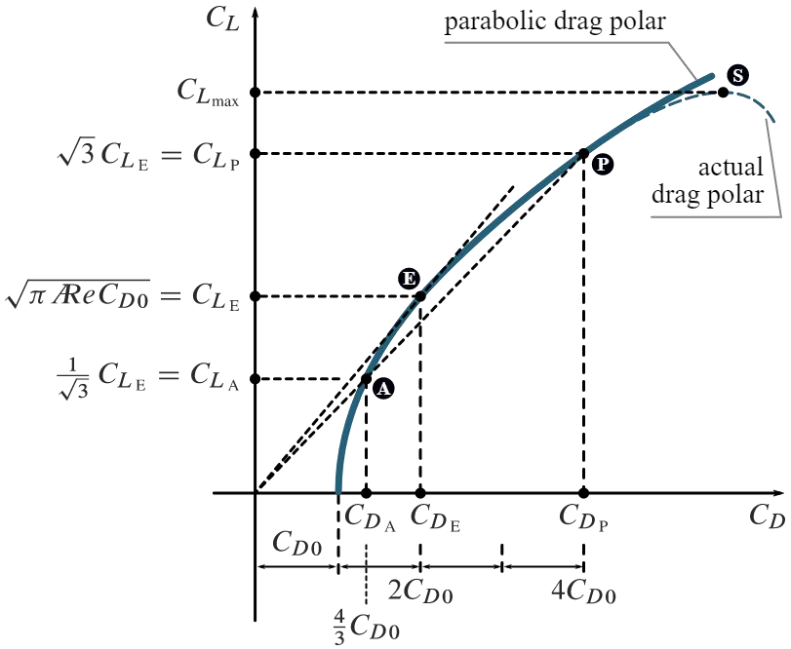

Fig. 3 Characteristic points E, P, and A on the parabolic drag polar.

Table 1 JPAD Modeller assumptions related to the estimation of the lift coefficients of the cruise, the alternate and the holding phase.

	CRUISE	ALTERNATE	HOLDING
JET	$C_L = C_{L_E} - \frac{2}{3}(C_{L_E} - C_{L_A}) = 0.718 \cdot C_{L_E}$	C_{L_E}	$C_L = C_{L_E} - \frac{1}{3}(C_{L_E} - C_{L_A}) = 0.859 \cdot C_{L_E}$
PROPELLER	$C_L = C_{L_E} - \frac{2}{3}(C_{L_E} - C_{L_A}) = 0.718 \cdot C_{L_E}$	$C_L = C_{L_E} - \frac{1}{2}(C_{L_P} - C_{L_E}) = 1.366 \cdot C_{L_E}$	$C_L = C_{L_E} - \frac{1}{3}(C_{L_E} - C_{L_A}) = 0.859 \cdot C_{L_E}$

These values of the lift coefficient are, then, used to compute the aircraft drag coefficient using the classical parabolic drag polar equation, from which the aerodynamic efficiency can be calculated.

JPAD Modeller estimates the aircraft zero-lift drag coefficient (C_{D0}) using the flap-plate analogy and starting from the equivalent skin-friction coefficient, a statistical value of the wing area and the statistical estimation of the aircraft wetted area based on the maximum take-off weight and the aircraft category.

In addition, the user has the possibility either to assign or to calculate Oswald factors related to all configurations. If calculated, the Oswald factor related to the clean configuration is estimated using the approach proposed by Torenbeek in [14]. Oswald factors for all other configurations are derived from the clean configuration assuming the offsets reported in Table 2.

Table 2 Assumptions related to the estimation of Oswald factors in take-off, landing and approach configurations

	OSWALD FACTOR OFFSET
TAKE-OFF	-0.05
LANDING	-0.1
APPROACH	-0.05

The possibility to calculate both aerodynamic efficiencies and Oswald factors represents an improvement with respect to typical conceptual design tools, which usually expects the user to assign them. This allows to increment the level of consistency of the generated aircraft model starting from the conceptual design phase.

After the preliminary weights estimation, JPAD Modeller allows to calculate all sizing limitations related to selected set or regulations (FAR-23 or FAR-25), the selected aircraft category and its type, to define the sizing plot, also known as matching point chart. Here the user is provided with an initial sizing point related to the statistically defined aircraft. However, this can be customized by the user using one of the following choices:

- **Maximum wing loading condition.**
- **Minimum engine requirement condition.**
- **User defined sizing point**, in this case the user can manually select the new sizing point from the matching point chart feasible zone.

Each time the sizing point is changed, JPAD Modeller updates the aircraft model accordingly and performs geometrical consistency checks on the following components:

- **Landing gears**, in terms positioning and geometrical parameters related to the main leg length and the wheel track.
- **The cabin layout**, to check if it fits current fuselage dimensions
- **Movables and control surface**, in terms of absolute and relative positioning.

In addition, since some sizing limitations and aerodynamic data relies on some key geometrical characteristics of the aircraft like the wing aspect ratio, the wing leading-edge sweep angle, the wing taper ratio and the winglet height, JPAD Modeller allows the user to manually override the statistically estimated values related to these parameters providing for more design flexibility.

An additional feature of JPAD Modeller, currently under development, is related to the extension of the PreDesign module to also include the conceptual design of hybrid-electric aircraft. This module, based on the work by Orefice *et.al.* [15], has been used in this work to design one of the aircraft models of the proposed joint workflow between JPAD Modeller and FlightStream®.

Once generated, the aircraft parametric model can be further refined with additional automatic CAD features as described in [12]. Those includes rounded lifting surface tips, winglets, pylons, fairings and movables (see Fig. 4).

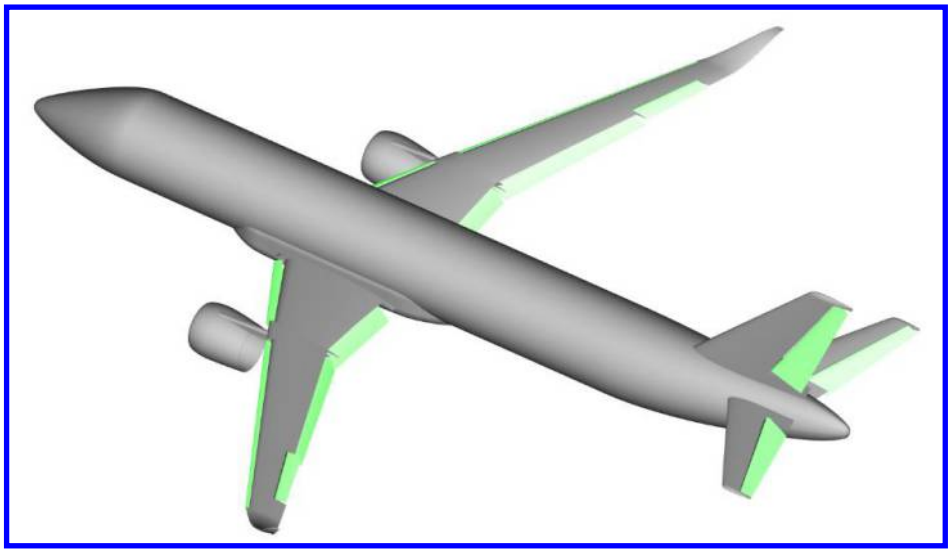

Fig. 4 JPAD Modeller aircraft with automatically generated movables

Furthermore, JPAD Modeller allows to parametrically customize nacelles and pylons to increase the level of detail of those components. In particular, four nacelle Levels Of Details (LOD) have been implemented (see Fig. 5):

- **LOD-0**: Generic nacelle shape. To be used for a simple nacelle representation starting from a small set of geometrical parameters. This is the only LOD available for propeller-driven engines.
- **LOD-1**: Simple turbofan nacelle. This LOD is available only for turbofan engines and allows to model the exit part of the engine.
- **LOD-2**: Ducted turbofan nacelle. This LOD, available only for turbofan engines, provides for more flexibility in terms of geometrical modelling of the nacelle shape which is represented as a duct. In fact, the inlet, the intake and the maximum diameter sections can be adapted to any shape the user needs thanks a flexible parametrical representation. This LOD can be used in interconnection with external aerodynamic commercial solvers (e.g., FlightStream®).
- **LOD-3**: Detailed turbofan nacelle. This LOD provides for the most detailed parameterization of a turbofan nacelle allowing to manage each internal component dimension. It has been designed to allow the user to produce and export a detailed turbofan model ready to be imported by external CFD analysis tools (e.g., StarCCM+).

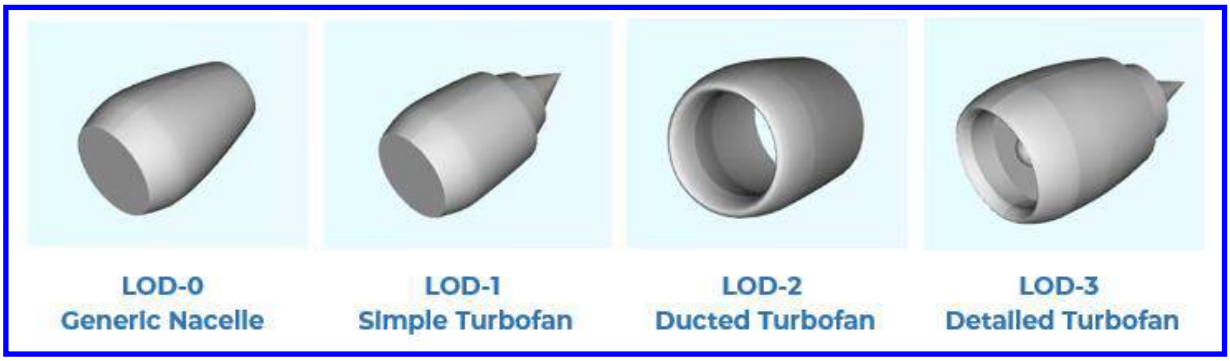

Fig. 5 JPAD Modeller nacelles levels of detail

The final part of the JPAD Modeller workflow is the exporting process of the aircraft. The tool allows to export both the aircraft CAD and the parametric model in several file formats including CPACS, the OpenVSP format VSP3 and the FlightStream® Component Cross Section (CCS) file. Thus, JPAD Modeller has all the features required to be a good pre-processor for aircraft preliminary design applications.

III. FlightStream

The mid-fidelity flow solutions for this effort were performed using the FlightStream® viscous surface-vorticity flow solver. As part of prior NASA SBIR 2018-20 funded activities, the Research in Flight company has developed the FlightStream® flow solver to make use of surface vorticity on an unstructured surface mesh to predict loads with attached flow [16][17]. Aerodynamic loads are computed by shedding vorticity from the geometry. The solver utilizes the Fast Multipole Method (FMM) [16]. The general implementation of FMM in any problem revolves around the coalescing of far-field potential inviscid source/doublet bodies into a single body for evaluation of the net effect on a near-field body [16]. The algorithm evaluates the inductive effect of near-field bodies identically to the $O(n^2)$ implementation but converts the large number of far-field bodies into a handful of clustered bodies inducting an effect based on the sum total of their field strengths. In FlightStream®, FMM implementation coalesces far-field vorticity into localized three-dimensional point doublets encompassing the net vorticity strengths of all of the coalesced far-field vorticity panels. Once the FMM near-field and far-field thresholds have been established, a spatial tree is constructed around the three-dimensional geometry to allow for the demarcation of these thresholds and to identify the near-field neighbors. The ideal spatial-tree for such an implementation is a spatial-octree. FlightStream® already uses an octree-based Cartesian mesh for propagating the wake strands. A similar implementation holds for the viscous formulation of surface vorticity. This allows extremely fast near-field sorting of points closest-to, or inside, a viscous flow region.

Two models for the boundary layer have been implemented: laminar and turbulent. A boundary layer transition model has also been implemented. All these models are two-dimensional methods implemented along the on-body surface streamlines. These integral methods are computationally efficient and can be applied to any general three-dimensional wall boundary with exceptions of regions involving three-dimensional crossflows. The laminar boundary layer analysis method used in FlightStream® is the standard two-parameter model of Thwaites [16] integral method

with the momentum integral equation. An integral boundary layer model for compressible turbulent flows has been implemented into the inviscid flow solver [16]. The final turbulent boundary layer model implemented has numerical improvements and optimizations over that of the original model developed by Standen, but philosophically follows the work of Standen quite closely, with the application to subsonic, turbulent, compressible flows along on-body streamlines. The method is essentially two-dimensional (similar to the laminar model described previously) but is implemented in a quasi-three-dimensional manner inside FlightStream®. For the fluid properties outside the boundary layer, the flow is assumed to be isentropic and subsonic, but compressible. Solving these equations numerically (using 4th order Runge-Kutta methods) along the on-body streamline generates all relevant turbulent boundary layer data. This data is then used to compute the boundary layer thicknesses.

With the addition of advanced viscous models, additional computational enhancements have been added to the solver to maintain an $O(nlog(n))$ scalability to the performance of the boundary layer algorithms. To this end, spatial octree algorithms that mimic the existing Fast Multipole Method implementation (for the inviscid solver) has been implemented for the viscous flow near-wall regions. This allows extremely fast near-field sorting of points closest-to, or inside, a viscous flow region. This spatial tree increases the memory footprint of the solver by roughly 5% for all cases. However, the performance benefits are substantial with an otherwise $O(n \times m)$ algorithm (where m is a very large number = solver surface mesh faces) being reduced to $O(nlog(n))$.

A robust model for computing attachment lines and critical points on the inviscid surface velocity fields generated in the solver was added. This is an enabling requirement for robust coupling with the viscous boundary layer models described previously. The laminar and turbulent boundary layer models were integrated with the inviscid solver via displacement of the inviscid boundary equal to the displacement thicknesses of the local boundary layers. For boundary layers, the displacement thickness indicates the extent to which the surface would have to be displaced in order to be left with the same flow rate of the viscous flow, but with an inviscid velocity profile. Therefore, the displacement thickness is suited for the measure of displacement needed for the inviscid boundary. The inviscid boundary displacement is simulated by blowing a velocity normal to the mesh face. The magnitude of the blowing velocity can be computed by using the momentum flux equations. This transpiration velocity can be computed along the on-body streamlines for each mesh face using standard finite-difference numerical marching schemes. The transpiration (blowing) velocity is then used to modify the inviscid Neumann boundary condition [16]. Main software innovations are highlighted in Table 3.

Table 3 Key innovations in FlightStream®

KEY INNOVATIONS IN FLIGHTSTREAM®
1. Unstructured surface meshes: no volume meshing required.
2. Actuator-based propeller modeling: multi-rotor simulations
3. Fast Multipole Method solver: very large mesh sizes (or multiple rotors with wakes) solved in minutes; no $\boldsymbol{O(n^2)}$ efficiency limitations in the potential flow solver.
4. Advanced wake proximity avoidance algorithms: automated and easy modeling of mutual interference of wakes as well as immersed lifting surfaces and bodies.
5. Non-linear solver capabilities: boundary layers, flow-separation.
6. Unsteady solver
7. Industry validated for Vertical Take-Off and Landing (VTOL) UAM applications.

IV. Aerodynamic solver validation and applications

FlightStream® has been extensively validated for DEP applications. Sample results are shown in Fig. 6 for the NASA XC-142 Quad-rotor VTOL aircraft [18]. The large propellers on this VTOL aircraft are modeled using the FlightStream® propeller actuator models for steady-flow analysis [18]. Results are shown for both the powered (thrust coefficient = 0.49) and unpowered configurations. The data is compared with the NASA experimental wind tunnel data [18]. The predicted onset of non-linearity in the lift forces as well as the CL_{MAX} predictions are found to be in good agreement for the unpowered configuration. The powered loads are also predicted with high accuracy [18].

Another case study illustrated in Fig. 7 and Fig. 8 is significant to the current effort. Fig. 7 shows the results from a recent validation work [19][20][21] performed for the NASA X-57 Scalable Convergent Electric Propulsion Technology and Operations Research (SCEPTOR) DEP aircraft. This geometry, as modeled in FlightStream®, is shown in Fig. 7. The X-57 has 12 high-lift propellers mounted on nacelles upstream of the wing leading edge that are positioned in an alternating fore- and aft-staggered pattern. The high-lift propellers are designed to fold smoothly onto the nacelle for the cruise configuration. These propellers were modeled using the propeller actuator models in FlightStream®. The nacelles and wing geometry were modeled with full fidelity from available CAD data.

Fig. 8 shows the results for the FlightStream® computed lift coefficient versus angle-of-attack (AOA) at a freestream Reynolds Number of 2.83 million and a Mach number of 0.233 [19]. Results are shown for the potential-flow solver mode in FlightStream® with the separation models enabled [16]. Comparison is provided with the NASA computational studies performed using the FUN3D Navier-Stokes flow solver. The computed lift coefficients for all range of incidence angles (including flow separation and stall) are in excellent agreement with available data. Fig. 8 shows similar results and trends for drag forces for the NASA X-57 Maxwell DEP aircraft. FlightStream® uses a post-stall drag model based on vortex shedding, which is particularly useful for such analysis. The post-separation forces predicted by FlightStream® are found to be within very reasonable error margins relative to the Navier-Stokes CFD solutions; and are a significant improvement over the existing potential-flow vortex-lattice methods.

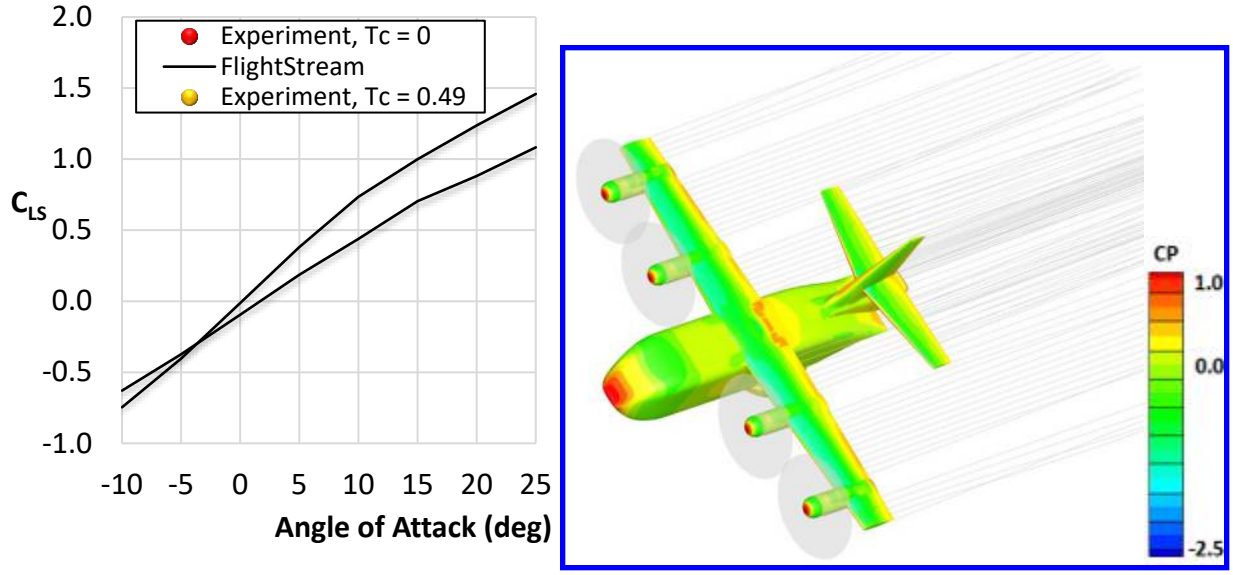

Fig. 6 FlightStream® slip-stream-corrected loads and surface pressure results for the NASA XC-142 V/STOL aircraft. Results shown for both the powered (yellow) and unpowered (red) configurations are shown.

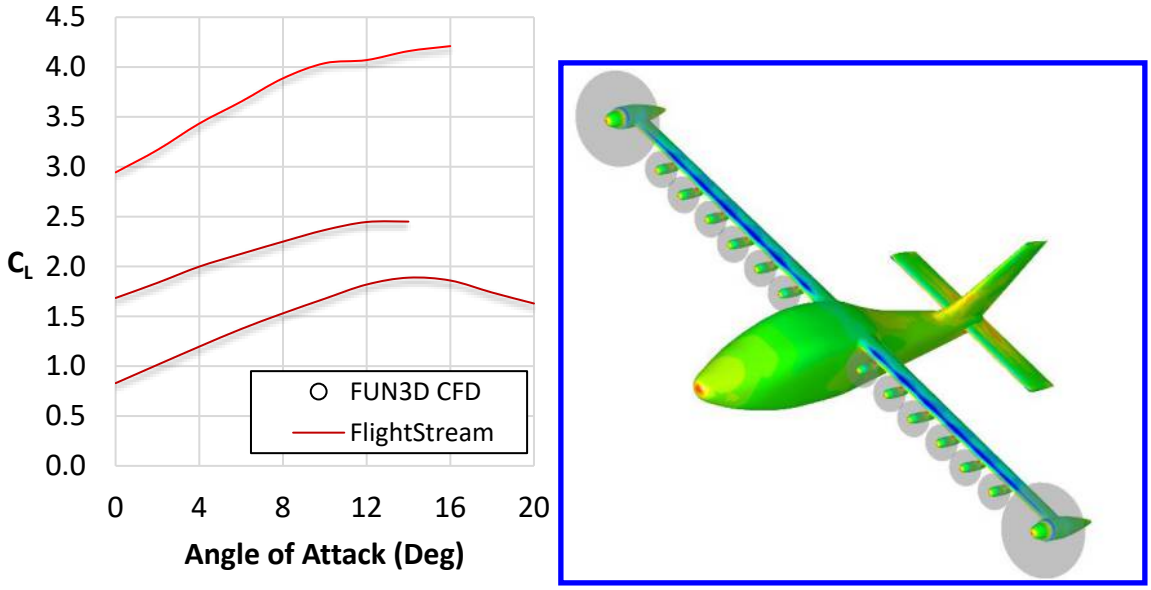

Fig. 7 FlightStream® lift coefficient forces and surface pressure results for the NASA X-57 Maxwell DEP aircraft. $Re = 2.83$ Million and $M = 0.233$. Results compared with CFD results published by NASA Langley using FUN3D Navier-Stokes Flow Solver. FlightStream® solver run-time is less than five minutes.

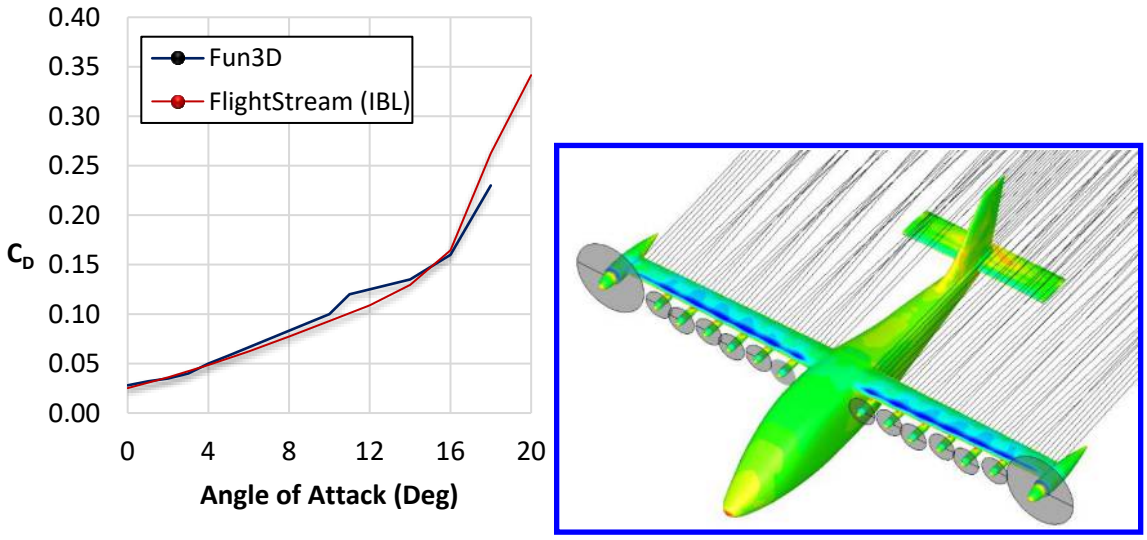

Fig. 8 FlightStream® post-separation drag coefficient for the NASA X-57 Maxwell DEP aircraft. Re = 2.83 Million and M = 0.233. Results compared with NASA Langley FUN3D CFD results.

V. Workflow implementation and results

In collaboration with the Research in Flight team, a workflow coupling JPAD Modeller and FlightStream® has been setup thanks to the joint development of the interface between the two software. This allows to really speed up the initial geometry generation and to receive fast and accurate feedbacks concerning the aircraft aerodynamics.

A case study using as reference aircraft a 19 passengers turboprop commuter is shown to describe the workflow. The initial aircraft geometry has been generated using JPAD Modeller and starting from the set of TLAR listed in Table 5. A first estimation of the aircraft weights and the definition of all performance limitations has allowed to define the feasible design zone on the sizing limitations plot, from which the sizing point related to the maximum wing loading (W/S) has been selected to generate the geometry. Then, the aircraft model has been automatically exported from JPAD Modeller to FlightStream® where a complete aerodynamic analysis has allowed to obtain reference data concerning total lift, total drag polar and total pitching moment curves of the aircraft.

At this point, a Distributed Electric Propulsion (DEP) configuration has been generated using a currently under development internal module of JPAD Modeller based on the statistical pre-design and the sizing workflow explained by Orefice *et.al.* [15]. This to simulate a typical workflow in which a designer should convert a conventional configuration to an innovative one, starting from a fixed set of TLAR, to investigate the behavior of the new aircraft. The set of input data for the DEP configuration, according to the workflow explained in [15], is shown in Table 6. Concerning each operating mode index reported in Table 6, they have been derived from the work by de Vries *et. al.* [22] and reported in Table 7. Furthermore, it is useful to report the definition of both the supplied power ratio Φ and the shaft power ratio φ which are related to the powertrain schema shown in Fig. 9.

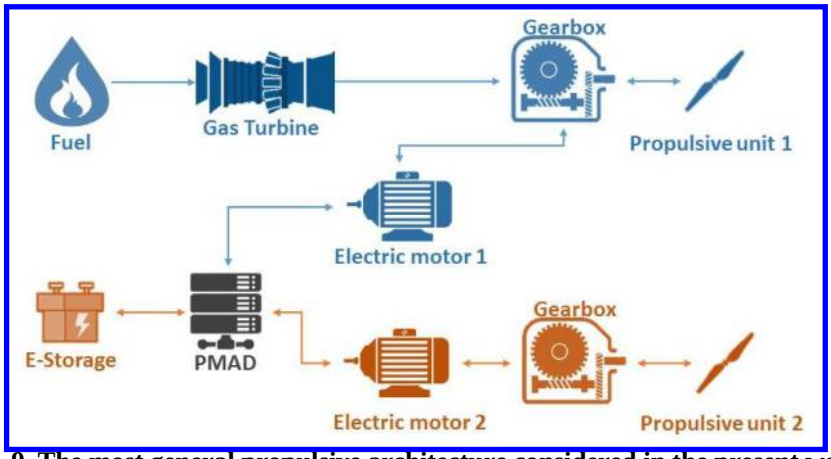

Fig. 9 The most general propulsive architecture considered in the present work.

$$\Phi = \frac{P_{\text{E-storage}}}{P_{\text{fuel}} + P_{\text{E-storage}}}$$

$$\varphi = \frac{P_{\text{prop 2}}}{P_{\text{prop 1}} + P_{\text{prop 2}}}$$

By using the same workflow, the new configuration has been automatically exported to FlightStream® and a new aerodynamic assessment has been carried out. Results in terms of sizing limitations plot are shown in Fig. 10.

A comparison between the two aircraft models is shown in Fig. 11. Both aircraft have been analyzed in powered conditions at take-off, where the effects coming from the DEP have the highest relevance. In addition, no high-lift devices have been considered, since the focus is on the pure aerodynamic effect coming from the DEP. To derive the operating conditions of each engine to be used inside FlightStream®, the following definition of the thrust coefficient C_T has been considered according to the FlightStream® user guide.

$$C_T = \frac{T}{\rho\, A_{disk}\, (\omega\, R_{disk})^2}$$

Starting from the baseline model, the thrust T of each engine has been derived from the JPAD Modeller engine deck considering a Mach number of 0.147 at sea level in standard ISA conditions. The propeller disk radius R_{disk} has been used to calculate the disk area A_{disk}. Finally, the rotation speed parameter ω has been calculated from the following equation and assuming 2200 RPM.

$$\omega = \frac{2\pi\, RPM}{60}$$

Operating conditions related to the DEP configuration have been obtained by considering that the overall aircraft thrust at take-off must be equal to the one coming from the selected design point. Knowing the number of both electric and thermal engines, as well as their geometrical characteristics in terms of propellers, the values of all thrust coefficients have been estimated by assuming that thermal engine propellers are working at 1600 RPM and that electric engine propellers are working at 2000 RPM. A summary of all engines operating conditions is provided in Table 4.

Table 4 Summary of engines operating conditions for FlightStream®

Conventional configuration	C_T	RPM
Engine 1	0.0234	2200
Engine 2	0.0234	2200
DEP configuration	**C_T**	**RPM**
Engine 1 – Thermal Engine	0.0149	1600
Engine 2 – Thermal Engine	0.0149	1600
Engine 3 – Electric Engine	0.0394	2000
Engine 4 – Electric Engine	0.0394	2000
Engine 5 – Electric Engine	0.0394	2000
Engine 6 – Electric Engine	0.0394	2000
Engine 7 – Electric Engine	0.0394	2000
Engine 8 – Electric Engine	0.0394	2000
Engine 9 – Electric Engine	0.0394	2000
Engine 10 – Electric Engine	0.0394	2000

Table 5 Set of Top-Level Aircraft Requirements for JPAD Modeller.

Description	Value	Unit
Configuration	High-Wing, Conventional Tail, Wing-mounted engines	
Aircraft type	Commuter	
Design passengers	19	
Number of pilots	2	
Design range	500	nmi
Number of engines	2	

Engine type	Turboprop	
Airport altitude	0	m
Landing field length	780	m
Take-off field length	800	m
Climb speed	170	kn
Rate of Climb	2150	ft/min
Cruise Mach number	0.317	
Cruise altitude	10000	ft
Descent speed	120	kn
Rate of Descent	700	ft/min
Alternate range	100	nmi
Alternate Mach number	0.28	
Alternate altitude	10000	ft
Holding duration	30	min
Holding Mach number	0.113	
Holding altitude	1500	ft

Table 6 Most relevant input parameters for the statistical pre-design and sizing of the DEP configuration

Description	Value	Unit
Powertrain architecture	Hybrid	
APU installed	No	
Operating mode (Take-Off)	1	
Operating mode (Climb)	1	
Operating mode (Cruise)	1	
Operating mode (Descent)	3	
Operating mode (Landing)	1	
Operating mode (Alternate cruise)	1	
Operating mode (Holding)	1	
Supplied power ratio, Φ (Take-Off)	0.1	
Supplied power ratio, Φ (Climb)	0.1	
Supplied power ratio, Φ (Cruise)	0.1	
Supplied power ratio, Φ (Descent)	0.1	
Supplied power ratio, Φ (Landing)	0	
Supplied power ratio, Φ (Alternate cruise)	0	
Supplied power ratio, Φ (Holding)	0	
Shaft power ratio, φ (Take-Off)	0.7	
Shaft power ratio, φ (Climb)	0.3	
Shaft power ratio, φ (Cruise)	0	
Shaft power ratio, φ (Descent)	0	
Shaft power ratio, φ (Landing)	0.7	
Shaft power ratio, φ (Alternate cruise)	0	
Shaft power ratio, φ (Holding)	0	
Thermal system type	Gas Turbine	
Number of secondary engines	8	
Wingspan occupied by DEP	70.1%	

Thermal engines propeller diameter	2.5	m
Electric engines propeller diameter	1.5	m
Distance between propellers	0.015	m
Tip Vortex Wing Control System	Counter-rotating secondary engines at tip	
Number of Battery Packs	2	
Minimum State of Charge	0.2%	
Specific Power of the Primary Electric Motor (EM1)	7.7	kW/kg
Specific Power of the Secondary Electric Motor (EM2)	7.7	kW/kg
Specific Power of the Battery	0.5	kW/kg
Specific Energy of the Battery	333	Wh/kg

Table 7. Hybrid-electric powertrain operating modes [22]. The operating mode of the electric motor 2 depends on that of propulsive unit 2, electric motor 1 and electric energy source (see Fig. 9).

	1	**2**	**3**	**4**	**5**	**6**	**7**	**8**	**9**
Propulsive unit 1	thrust	thrust	thrust	thrust	thrust	thrust	harvest	harvest	harvest
Propulsive unit 2	thrust	thrust	harvest	thrust	harvest	harvest	thrust	thrust	harvest
E-Storage	discharge	charge	charge	discharge	discharge	charge	discharge	charge	charge
Electric Motor 1	generator	generator	generator	motor	motor	motor	generator	generator	generator

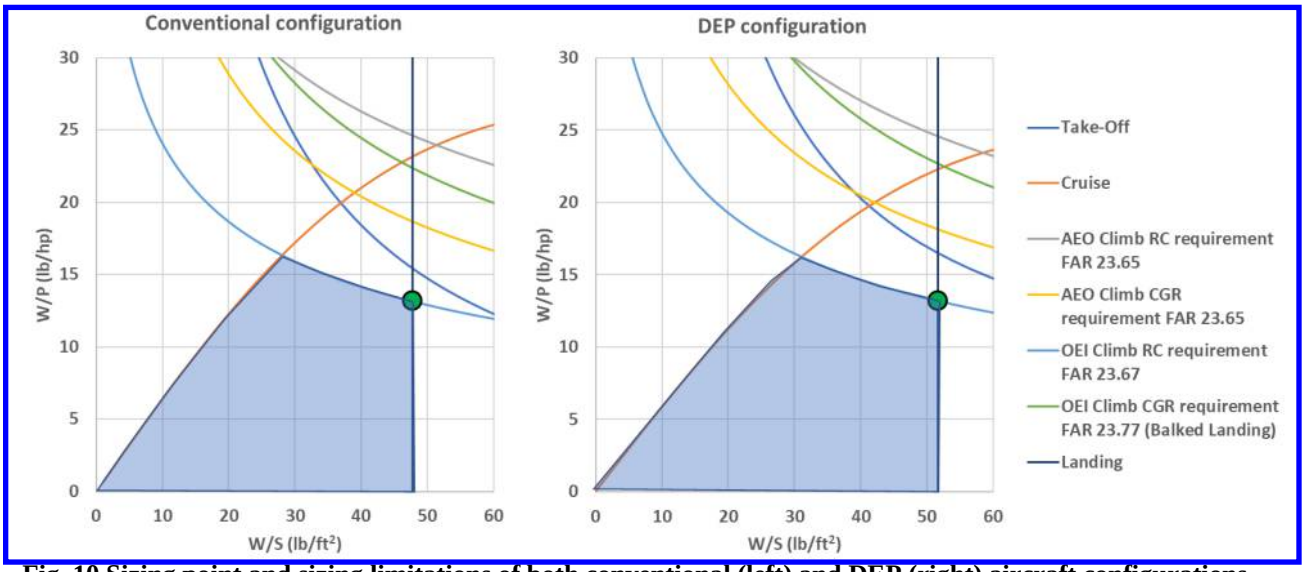

Fig. 10 Sizing point and sizing limitations of both conventional (left) and DEP (right) aircraft configurations using JPAD Modeller

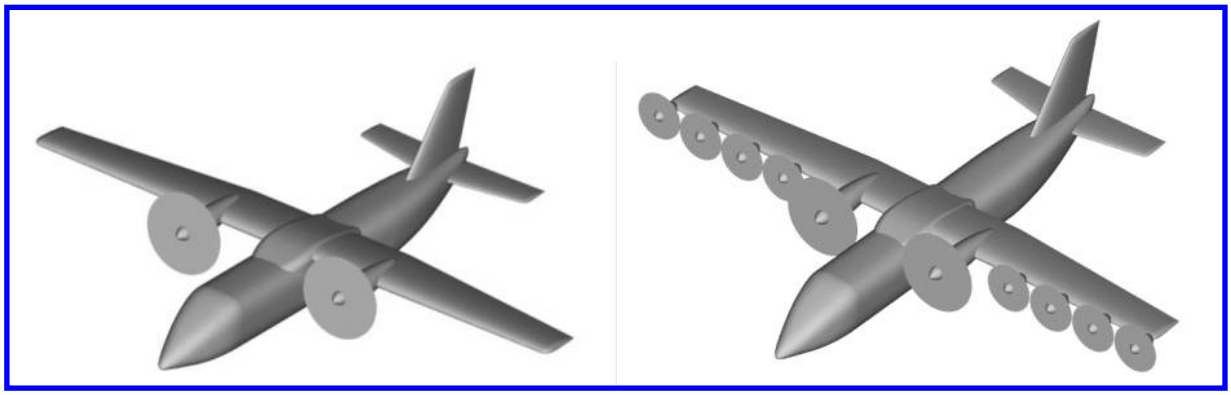

Fig. 11 Conventional and DEP turboprop commuter aircraft configurations generated using JPAD Modeller

By using the JPAD Modeller interface with the FlightStream® software, an aerodynamic comparison between the two configurations has been carried out. Fig. 12 highlights the effect of the wing blowing which causes an increment in maximum lift coefficient of about 0.531 with respect to the baseline value of 1.22.

The conventional configuration stalls at an angle of attack of 16° at a Reynolds number of 6.19 million, while the DEP configurations encounter vehicle stall at a flow incidence angle of 18° at a Reynolds Number of 6.81 million.

The drag coefficient chart reported in Fig. 13 allows to estimate the drag increment related to the introduction of the DEP. Although the induced drag coefficient increment is the most relevant contribution, there is also a slight increment of the parasite drag coefficient which can be addressed to the variation in friction coefficient caused by the adoption of the DEP configuration.

It must be noted that the DEP wing planform area has changed from the baseline wing of only few square meters (about -3m^2) while keeping the same wingspan. Thus, the expected increment in lift coefficient due to the blowing effect of the DEP architecture has led to a higher induced drag coefficient, not countered by the very little increment in wing aspect ratio. This, has provided for a slightly lower value of the aerodynamic efficiency in this flight condition, as shown in Fig. 14.

Finally, both vehicles are also statically stable, as shown in Fig. 15. Here, the reference point for all moments has been assumed equal the 25% of the Mean Aerodynamic Chord (MAC). The comparative analysis has also highlighted the increment in pitching moment due to the adoption of the DEP propulsive architecture at low angles of attack.

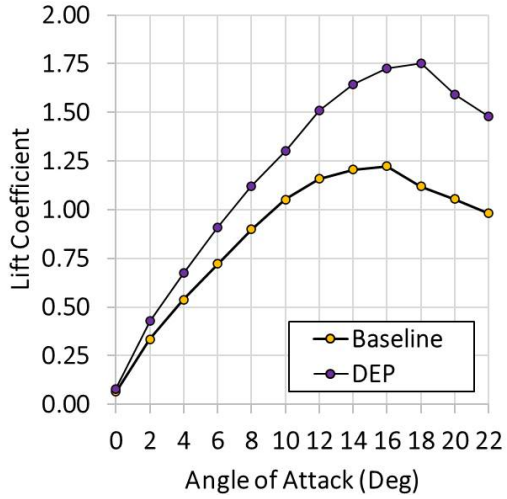

Fig. 12 FlightStream® flow solutions: Lift coefficient versus angle of attack for the conventional and the DEP configurations Mach 0.147, Sea Level, ISA Condition, Re=6.19M (Baseline), Re=6.81M (DEP).

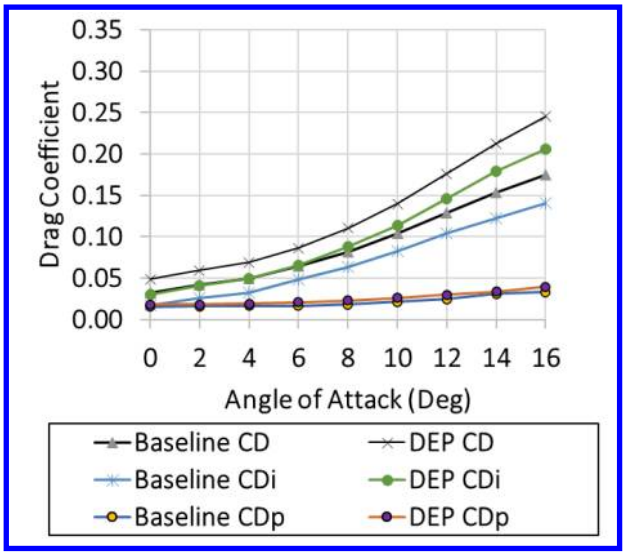

Fig. 13 FlightStream® flow solutions: Drag coefficient versus angle of attack for the conventional and the DEP configurations at Mach 0.147, Sea Level, ISA Condition, Re=6.19M (Baseline), Re=6.81M (DEP).

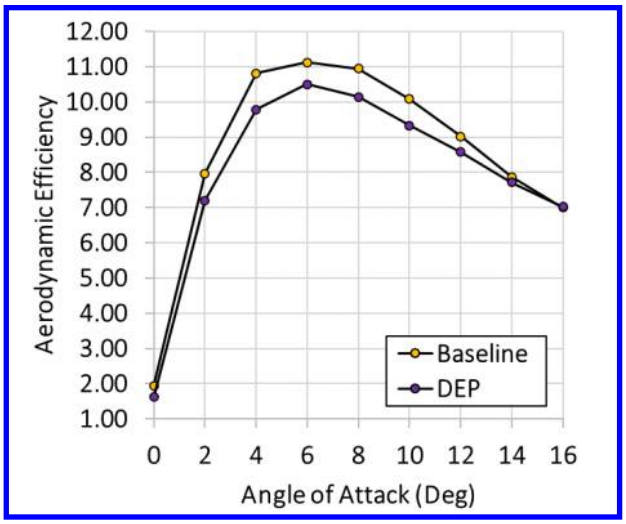

Fig. 14 FlightStream® flow solutions: Aerodynamic efficiency versus angle of attack for the conventional and the DEP configurations at Mach 0.147, Sea Level, ISA Condition, Re=6.19M (Baseline), Re=6.81M (DEP).

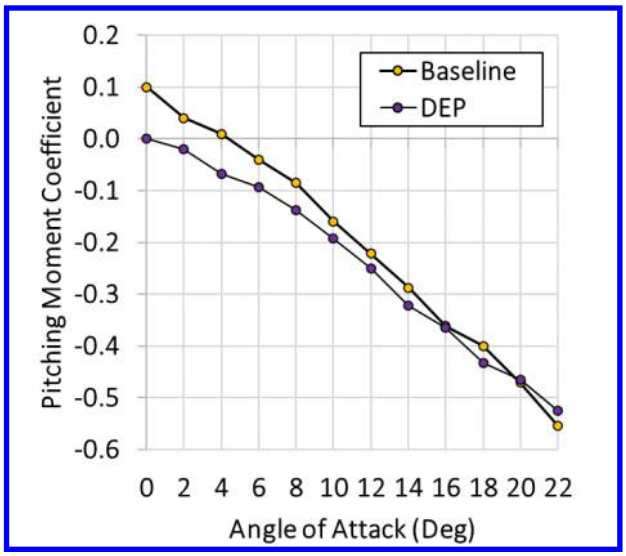

Fig. 15 FlightStream® flow solutions: Pitching moment versus angle of attack for the conventional and the DEP configurations Mach 0.147, Sea Level, ISA Condition, Re=6.19M (Baseline), Re=6.81M (DEP).

All JPAD Modeller tasks have been executed on laptop PC with 32 Gb of RAM and an octa-core Intel Core i7-10875H processor. A breakdown of the computational times required for all tasks is reported in Table 8. In addition, FlightStream® simulations were run on a standard quad-core PC workstation and had a solver runtime measured at about 30 seconds per simulation run. The full sweep of results shown from Fig. 12 to Fig. 15 required 7.3 minutes to complete for each configuration. However, this time may be further reduced by adopting a parallelized approach.

Table 8 Summary of the computational times for all case study tasks.

Task	Adopted tool	Computational time	Notes
Baseline geometry generation	JPAD Modeller	8.0 seconds	Including preliminary weights estimation and sizing plot definition (iterative process)
Complete aircraft model and CAD generation	JPAD Modeller	30.4 seconds	
Baseline geometry export to FlightStream®	JPAD Modeller	10.0 seconds	

Complete aerodynamic assessment of the baseline aircraft model	FlightStream®	7.3 minutes	Including lift, drag and pitching moment calculations for each angle of attack and using the viscous-coupling feature for computing the boundary layer effects and the stall prediction.
Generation of the DEP configuration	JPAD Modeller	56.2 seconds	Including statistical pre-design and sizing according to [15]
Complete DEP aircraft model and CAD generation	JPAD Modeller	52.3 seconds	The time increment is due the increased number of engines
DEP configuration export to FlightStream®	JPAD Modeller	26.3 seconds	The time increment is due the increased number of engines
Complete aerodynamic assessment of the DEP configuration aircraft model	FlightStream®	7.3 minutes	Including lift, drag and pitching moment calculations for each angle of attack and using the viscous-coupling feature for computing the boundary layer effects and the stall prediction.
Total workflow time		**17.65 minutes**	

VI. Conclusions

This work has shown that in less than 20 minutes the integrated workflow implemented using JPAD Modeller and FlightStream® has allowed to obtain useful and reliable preliminary design feedbacks concerning the effects of a distributed electric propulsion architecture applied on a conventional turboprop commuter aircraft automatically generated starting from a simple set of TLAR, mission profile data and aerodynamic assumptions. Thus, the provided case study has proved that JPAD Modeller and its native exporting features towards external analysis tools like FlightStream® can effectively speed up typical design tasks increasing the designer level of knowledge since the conceptual and preliminary design phases.

References

[1] Trifari, V., Ruocco, M., Cusati, V., Nicolosi, F., and De Marco, A., "Multi-disciplinary analysis and optimization Java tool for aircraft design," *ICAS 31st Congress of the International Council of the Aeronautical Sciences*, Belo Horizonte, Brazil, 2018, ISBN: 9783932182884.

[2] Prakasha1, P.S., Ciampa, P.D., Della Vecchia, P., Ciliberti, D., Voskuij, M., Charbonnier, D., Jungo, A., Zhang, M., Fioriti, M., Anisimov, K. and Mirzoyan, A., "Model Based Collaborative Design & Optimization of Blended Wing Body Aircraft Configuration: AGILE EU Project". *AIAA Aviation and Aeronautics Forum and Exposition (AIAA Aviation)*, Atlanta, Georgia, 2018. DOI: 10.2514/6.2018-4006.

[3] Research in Flight Company, FLIGHTSTREAM®, 2020, url: https://researchinflight.com/products.html, [Accessed: 18/10/2021].

[4] Dassault Systèmes, DISCOVER CATIA, 2021, url: https://www.3ds.com/products-services/catia/, [Accessed: 18/10/2021].

[5] Dassault Systèmes SolidWorks Corporation, 2021, url:https://www.solidworks.com/ [Accessed: 18/10/2021].

[6] National Aeronautics and Space Administration NASA, OpenVSP, 2021, url: http://openvsp.org/, [Accessed: 18/10/2021].

[7] Drougard, M., CPACS Creator, 2019, url: https://dlr-sc.github.io/tigl/cpacs-creator-pre-release.html [Accessed 18/10/2021].

[8] Deutsches Zentrum für Luft- und Raumfahrt e.V. (DLR), 2018, COMMON LANGUAGE FOR AIRCRAFT DESIGN, url: https://www.cpacs.de/ [Accessed: 18/10/2021].

[9] De Marco, A., Cusati, V., Trifari, V., Ruocco, M., Nicolosi, F. and Della Vecchia, P., "A Java Toolchain of Programs for Aircraft Design", *Proceedings of the 6th CEAS Air and Space Conference*, Bucharest, Romania, 2017, ISBN: 978-973-0-25597-3.

[10] Trifari, V., Ruocco, M., Cusati, V., Nicolosi, F., and De Marco, A. "Java Framework for Parametric Aircraft Design – Ground Performance". *Aircraft Engineering and Aerospace Technology (AEAT)*, Vol. 89, No. 4, 2017, pp. 599–608, doi: http://dx.doi.org/10.1108/AEAT-11-2016-0209.

[11] Nicolosi, F., De Marco, A., Attanasio, L., and Della Vecchia, P., "Development of a Java-based framework for aircraft preliminary design and optimization*," AIAA Journal of Aerospace Information Systems*, Vol. 13, No. 16, 2016, pp. 234-242, doi: https://doi.org/10.2514/1.I010404.

[12] De Marco, A., Di Stasio, M., Della Vecchia, P., Trifari, V., and Nicolosi, F., "Automatic modeling of aircraft external geometries for preliminary design workflows". *Aerospace Science and Technology*, Vol. 8, 2020. doi: 10.1016/j.ast.2019.105667.

[13] Loftin, L. K., & Langley Research Center, “Subsonic aircraft: Evolution and the matching of size to performance”, Washington, D.C: National Aeronautics and Space Administration, Scientific and Technical Branch, 1980.
[14] Torenbeek, E. *Advanced Aircraft Design - Conceptual Design, Analysis and Optimization of Subsonic Civil Airplanes*. John Wiley & Sons, Chicester, UK, 2013, Chap. 4.
[15] Orefice, F., Della Vecchia, P., Ciliberti, D., Nicolosi, F., “Aircraft Conceptual Design Including Powertrain System Architecture and Distributed Propulsion”, *2019 AIAA/IEEE Electric Aircraft Technologies Symposium (EATS)*, Indianapolis, USA, 2019, doi: 10.2514/6.2019-4465.
[16] Burkhalter, J.E., Ahuja, V., Hartfield R., “Robust prediction of high lift using surface vorticity”, NASA SBIR NNX17CL12C, Phase II final report, 2017
[17] Ahuja V., and Hartfield R. J., "Aerodynamic Loads over Arbitrary Bodies by Method of Integrated Circulation", *Journal of Aircraft*, Vol. 53, No. 6 (2016), pp. 1719-1730.
[18] Sandoz B., Ahuja V., and Hartfield R. J., "Longitudinal Aerodynamic Characteristics of a V/STOL Tilt-wing Four-Propeller Transport Model using a Surface Vorticity Flow Solver", *2018 AIAA Aerospace Sciences Meeting, AIAA SciTech Forum*, (AIAA 2018-2070)
[19] Deere, K. A., Viken, S. A., Carter, M. B., Viken J. K., Derlaga J. M., “Comparison of High-Fidelity Computational Tools for Wing Design of a Distributed Electric Propulsion Aircraft”, *35TH AIAA Applied Aerodynamics Conference*, 5-9 June 2017. AIAA-2017-3925.
[20] Viken J. K., Viken, S. A., Deere, K. A., Carter, M. B., “Design of the Cruise and Flap Airfoil for the X-57 Maxwell Distributed Electric Propulsion Aircraft”, *35TH AIAA Applied Aerodynamics Conference*, 5-9 June 2017. AIAA-2017-3922.
[21] Deere, K. A., Viken J. K., Viken, S. A., Carter, M. B., “Computational Analysis of a Wing Designed for the X-57 Distributed Electric Propulsion Aircraft”, *35TH AIAA Applied Aerodynamics Conference*, 5-9 June 2017. AIAA-2017-3923.
[22] de Vries, R., Brown, M.T., and Vos, R., “A Preliminary Sizing Method for Hybrid-Electric Aircraft Including Aero-Propulsive Interaction Effects,” *2018 Aviation Technology, Integration, and Operations Conference*, Atlanta, Georgia, USA, 2018. doi:10.2514/6.2018-4228.c1.

***